Available online at www.sciencedirect.com
SCIENCE DIRECT®
Computerized Medical Imaging and Graphics 27 (2003) 459–467
Computerized Medical Imaging and Graphics
www.elsevier.com/locate/compmedimag

Hand bone segmentation in radioabsorptiometry images for computerised bone mass assessment

José M. Sotoca[a,1], José M. Iñesta[b,*], Miguel A. Belmonte[c]

[a]Dpto. de Lenguajes y Sistemas Informáticos, Universidad Jaume I, Campus Riu Sec, E-12071 Castellón, Spain
[b]Department de Lenguajes y Sistemas Informáticos, Universidad de Alicante, Apartado 99 Alicante E-03080, Spain
[c]Unidad Reumatología y Bioinformática, Hospital General de Castellón, E-12004 Castellón, Spain

Received 6 November 2002; accepted 9 April 2003

Abstract

From hand radiographs, the measurement of the bone density of hand bones is automatically performed, using units relative to an aluminium wedge, in order to know the absorption of the ray light intensity respect to a known substance. By means of a point distribution model, the variation modes of a statistical model of the phalanx are determined, and the boundaries of such bones localised, aiming to obtain their average grey level. The goal is to obtain an accurate and reliable computerised radiographic X-ray absorptiometry system for automatic bone mass assessment that can be easily applied to the population. The developed system has been tested and compared to other known methods with a high level of correlation.

Keywords: Image segmentation; Active shape models; Medical imaging; Osteoporosis; Bone density

1. Introduction

The modern concept of osteoporosis emerged during the Copenhagen Conference [1], as an illness defined by a low bone mass and the deterioration of the bone micro-architecture causing a higher risk of fracture. Although the determination of the bone mass by physical ways does not evaluate the micro-architecture, and despite the fact that there are other causes which could hasten the formation of fractures, several studies have established the predictive factor of such determination for the posterior development of fractures [2].

Among the different quantitative techniques for bone mass determination, the most important ones are: simple photon absorptiometry (SPA), dual photon absorptiometry (DPA), and dual energy X-ray absorptiometry (DXA), being the latter the most extended. It is based on the creation of an image due to the attenuation of two X-ray spots, with high and low energies, over a determined anatomic area. The most important drawbacks of these high precision techniques are the high cost of the equipment and the few of them that can be found, usually centralised in the main cities. These facts limit the preventive and surveillance medical task over risk population sectors. Because of that, it is necessary the development of a reliable, inexpensive and simple measurement system. Radiographic absorptiometry systems fulfil these three conditions, as just from a single radiography it is possible to determine the bone mass in a reliable and reproducible way. This approach was proposed in Ref. [3] and some works have been devoted to study the feasibility of this method [4,5], mainly focused on the measurement of hand bone anatomical parameters, like metacarpal cortical thickness or diameter of the second metacarpal. The results have shown high correlations to DXA measurements under normal and pathological conditions [4–9].

A high standard of automation for a system to be applied for screening over a large population is required. The main problem for achieving this goal is the automatic segmentation of the bones of interest from digital radiographs. This problem has proved to be extremely challenging. A number of works on osteoporosis dealing with digital radiographs

* Corresponding author. Tel.: +34-965-90-3772; fax: +34-965-90-9326.
E-mail addresses: inesta@dlsi.ua.es (J.M. Iñesta), sotoca@lsi.uji.es (J.M. Sotoca), belmonte@ser.es (M.A. Belmonte).
[1] Tel.: +34-964-72-8359; fax: +34-964-72-8435.

0895-6111/03/$ - see front matter © 2003 Elsevier Ltd. All rights reserved.
doi:10.1016/S0895-6111(03)00053-3

analyse the regions of interest (ROI) in the image after selecting these ROIs by hand [10,11].

Some other works have dealt with the problem of automatic segmentation of hand radiographs applying it for assessing skeletal maturity [12–14] or arthritis [15]. Most of these works develop methods for segmentation based on region analysis [13,14] or methods based in the classification of given regions either using neural networks [12] or Bayesian models [15]. The works more related to osteoporosis, focus either on analysis of the trabecular bone structure [16–18] or on the assessment of the bone mineral density [18]. Some approaches have been developed like the use of fractal texture analysis in order to segment automatically trabecular bone structure [16] or the segmentation of the ROIs by means of adaptive thresholding for studying this structure in those segmented regions [17].

The purposes of this work are: (1) to design a robust system to segment automatically hand bones in digitised hand radiographs with a variability in the average grey level determination in the segmented area lower than 2%. For this, a point distribution model (PDM) will be generated from a set of training bone shapes. This model will be used for adaptation to the border of each instance of the bones in the images permitting that standard of precision; (2) to measure the bone density for the segmented hand bones using the grey levels calibrated with a reference aluminium wedge; (3) to design an accurate and reliable computerised radiographic X-ray absorptiometry system (CRXA) for automatic bone mass assessment that can be easily applied to the population; and (4) to validate the system and compare the results to other techniques and assess its diagnosis validity.

This paper is structured as follows: first, Sections 2 and 3 are provided on the theoretical framework used for segmentation; then the problems that arise for bone mass assessment are discussed; after that, the results on system validation and comparison to other techniques are provided and finally conclusions are drawn.

2. Point distribution and active shape models

PDM [19] are statistical models obtained from a set of examples. They are able to change their shape according to the possible deformations allowed in that *training set*. This ability is of a high value when dealing with biomedical shapes. The training set contains different examples of the shape to be modelled (here, a given metacarpal bone) and each example is represented by a set of labelled points in the shape contours, sufficient in number to characterise the object shape. The set of examples forms the PDM that reflects the variations of the shapes in that training set.

In order to make a statistical model from the shapes in the training set it is necessary to compare equivalent points among them. This process involves an alignment phase among the shapes: scale by a factor s, rotation by an angle θ and translation by a vector $\mathbf{t} = (t_x, t_y)$, with the purpose of minimising the weighted sum of square distances between equivalent points on different shapes. For aligning two shapes, the expression to be minimised is

$$E = (\mathbf{p}_{\text{ref}} - M(\mathbf{p}) - \mathbf{t})^T W(\mathbf{p}_{\text{ref}} - M(\mathbf{p}) - \mathbf{t}) \tag{1}$$

where the vectors $\mathbf{p}_{\text{ref}}$ and $\mathbf{p}$ contain the co-ordinates of the points of the reference object and those of the one that we want to align. M is the transformation matrix for aligning the vector $\mathbf{p}$ to $\mathbf{p}_{\text{ref}}$

$$M\left(\begin{bmatrix} x_i \\ y_i \end{bmatrix}\right) = \begin{bmatrix} (s\cos\theta)x_i - (s\sin\theta)y_i \\ (s\sin\theta)x_i + (s\cos\theta)y_i \end{bmatrix}, i = 1,\ldots,N \tag{2}$$

where N is the number of shape examples in the training set, and W is a diagonal matrix of statistical weights for each point in order to give more significance to those points that tend to be more stable over the set. If R_{kl} is the distance between two corresponding points in the set $\mathrm{d}(\mathbf{p}_k, \mathbf{p}_l)$ and $V_{R_{kl}}$ is the variance of those distances over the training set, the component w_k of the statistical weight matrix is

$$w_k = \left(\sum_{l=1}^{N} V_{R_{kl}}\right)^{-1}, \; k = 1,\ldots,N \tag{3}$$

So we have low weights if the sum of variances is large and vice-versa.

Once aligned, a mean shape $\bar{\mathbf{p}}$ is obtained. From each shape in the training set, $\mathbf{p}_i$, the deviation respect to the mean $\mathrm{d}\mathbf{p}_i = \mathbf{p}_i - \bar{\mathbf{p}}$ is computed and the covariance matrix, C, is obtained using

$$C = \frac{1}{N}\sum_{i=1}^{N} \mathrm{d}\mathbf{p}_i \mathrm{d}\mathbf{p}_i^T \tag{4}$$

Applying principal component analysis over C, the eigenvalues λ_k are obtained, providing the main modes of variation and what influence has each one of them in the distortion of the mean shape. Table 1 shows the values for λ_k (in proportion to the sum of all the eigenvalues) and the accumulated eigenvalues obtained from our training set of proximal phalanxes.

Table 1
Main variation modes and their eigenvalues in proximal phalanxes

Modes	$(\lambda_k/\lambda_{\text{total}}) \times 100$	Accumulated values
1	32.4	32.4
2	17.6	50.0
3	14.2	64.2
4	5.9	70.1
5	4.6	74.7
6	3.5	78.2
7	3.1	81.3

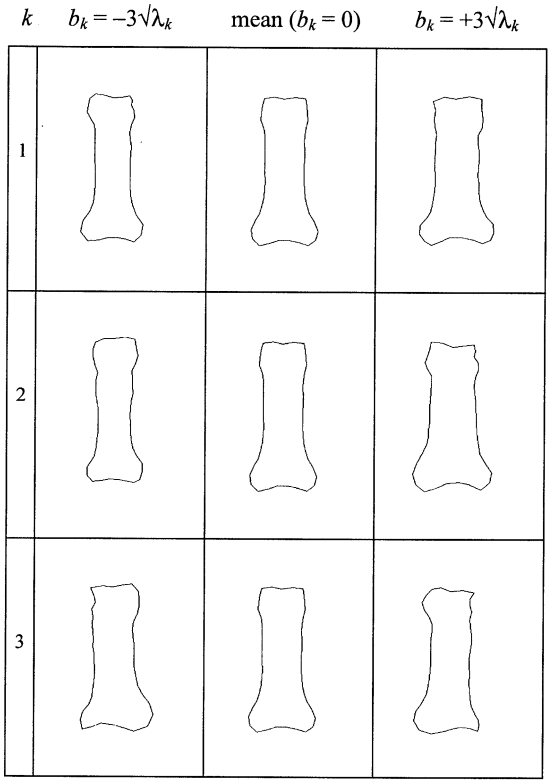

Fig. 1. Plot of the first three modes of variation for proximal phalanxes.

Any shape in the training set can be reconstructed from the main components of a PDM using this expression

$$\mathbf{p} = \bar{\mathbf{p}} + P_k \mathbf{b} \tag{5}$$

P_k is the matrix whose columns are the first k eigenvectors of C, and $\mathbf{b}$ is a vector of weights for those k eigenvectors. Also, any shape similar to those in the training set, can be approached varying the values of the components b_k of $\mathbf{b}$ within a suitable range, usually of the order of $\pm 3\lambda_k$. The value 3 is an amplification constant, c, heuristically set to increase the mobility of the model points. The variations of the model in order to reconstruct any desired shape is what is called the active shape model (ASM).

In Fig. 1, the effects of varying b_k for $k = 1, 2, 3$ across the above mentioned range are shown. The variation of each parameter represents a mode of variation of the shape. Thus, *mode* 1 seems to be related to the phalanx thickness, *mode* 2 to longitudinal variations and a widening of the phalanx condyles, and *mode* 3 to whether the phalanx corresponds to a left or right hand.

3. Location of the bone edges

We have worked with a number of points higher than 40 for all the shapes, enough for a good definition of their contours. Three different PDM of hand bones have been built, using 42 points for medial phalanxes, 47 points for proximal phalanxes, and 56 points for metacarpus bones. We have observed that, in distances less than 20 pixels between neighbour points of the model, the variability is small and good results are achieved.

The images have been scanned with a high-resolution scanner. This means that when using the gradient images to lead the ASM to the actual border, the internal texture of the bone can provide higher gradient values than those of the border. This problem is solved smoothing the gradient images and using this new image for the convergence of the model (Fig. 2).

An important factor that helps to make the convergence for segmentation easier is the use of rigidly adjusted templates (RAT) to determine what the finger orientation angle θ_{ref} is [20]. In this case, the template will be a rectangle with the same width as the finger and a height of 1.5 its width. The centre of the template is placed (with

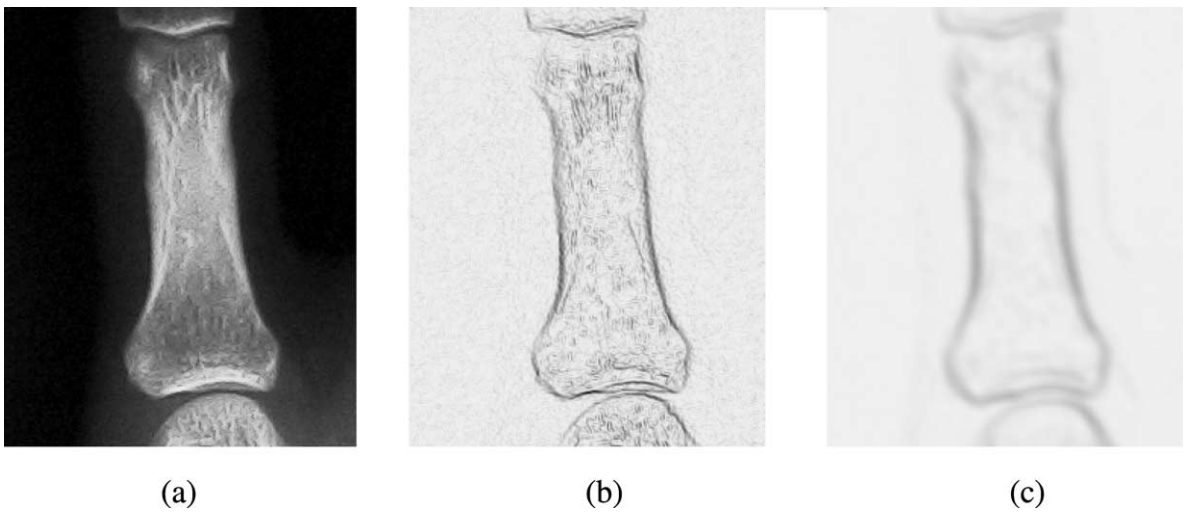

Fig. 2. (a) Original image of a medial phalanx. (b) Gradient image after applying a Sobel filter. (c) The same gradient image after applying a smoothing filter.

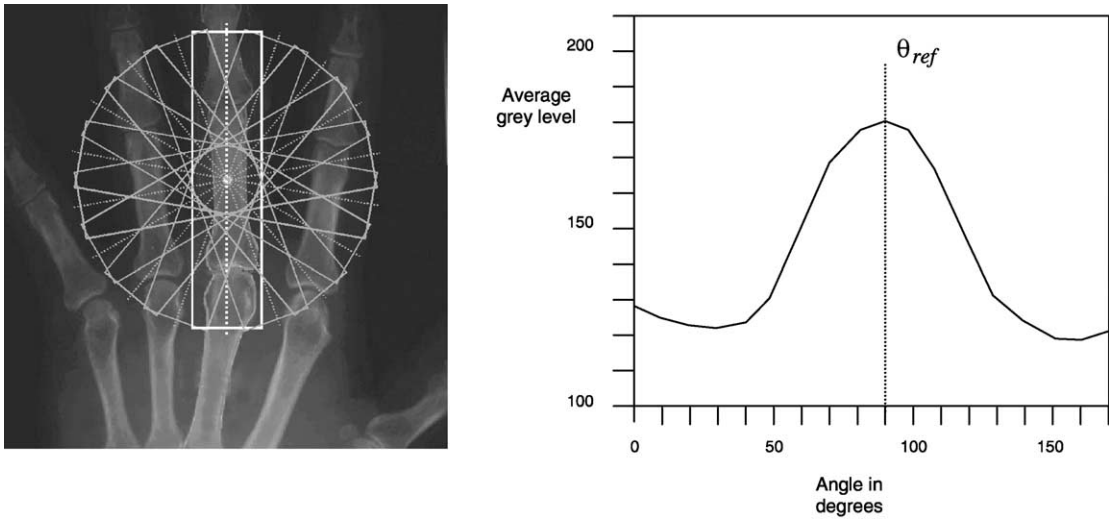

Fig. 3. Average grey level dependence in the template as a function of its orientation.

a click of the mouse) on the selected bone and the template is oriented in different angles from 0° to 170° and for each angle the average grey level inside the rectangle is assessed, obtaining a maximum value that provides θ_{ref} as shown in Fig. 3.

In addition, one constraint on the active curve is introduced: a rotation $(\theta - \theta_{\text{ref}})$ is applied to the evolving curve at each iteration. For determining the model rotation at each iteration respect to the reference angle θ_{ref}, we compute the angle θ between the minimum inertia axis of the shape and the horizontal axis of the image, using shape central moments, μ_{ij} and Eq. (6)

$$\theta = \frac{1}{2}\arctan\frac{2\mu_{11}}{\mu_{20} - \mu_{02}} \tag{6}$$

Once the bone orientation is determined, the minimum inertia axis of the ASM is aligned to θ_{ref} and the segmentation procedure begins. At each iteration, each point in the model moves along the normal to the model boundary, proportionally to the maximum grey level gradient $|\nabla I(x, y)|$ and towards the local maximum, looking for edge candidate points. These local transformations are transformed into adjustments in the pose, scale and shape parameters of the PDM [19], ensuring that the resulting shape remains similar to those in the training set. This procedure is iterated until no significant change results.

At each iteration, the active curve orientation is computed and it is aligned to that of the finger. This way we can guide its evolution towards a shape with favourable orientation to the bone we want to segment.

During the convergence process, an error function is defined that has to be minimised

$$E(\mathbf{t}, \theta, s, \mathbf{b}) = \sum_{k=1}^{2K} \|\mathbf{p}_{\text{g}} - E_k\|^2 + cD(\mathbf{b}) \tag{7}$$

This expression combines two terms: the first one is related to an external energy of the model as a function of the distance between the candidate points $\mathbf{p_g}$ and the transformation of the model in translation, rotation and scale E_k over the first K modes defined in the Eq. (1). The second term is an internal energy related to the change in the shapes at each iteration from the mean shape, being c an amplification constant and $D(\mathbf{b})$ a distance defined by Eq. (8)

$$D^2(\mathbf{b}) = \sum_{k=1}^{K} \frac{b_k^2}{\lambda_k} \tag{8}$$

The curve will extend or contract according to the variability of the model, aiming to reduce the distance between the PDM points and the bone boundaries, preserving the shape along the process. If the model does not find a variation mode able to reduce the distance, the amplification constant of movement variation, c, is reduced until it converges. The advantage of ASM with respect to other deformable models like *snakes* [21] is that the shapes to be segmented do not need to be smooth and in our experiments less error was achieved in the case of selecting wrong candidate points during the process.

4. Bone mass assessment

The method begins with the radiography of the non-dominating hand. A distance from the source to the plate is 1 m. The first thing to do in order to achieve valuable information out of the digitised radiograph is to calibrate the grey levels present on it. For this an aluminium wedge is placed on the plate, beside the hand, both in standardised positions, during the X-ray exposition. Now we will

describe the procedure to do this and discuss the problems that arise.

A photon beam with incising intensity I_0 that penetrates in a medium suffers an exponential attenuation as a function of the linear absorption coefficient of the medium, μ, and of the traversed thickness, t (measured here in cm), according to the law: $I = I_0 \exp(-\mu t)$. A change of variable can be made in order to establish this attenuation law as a function of the mass per area (in g/cm^2), $x = \rho t$, where ρ is the density. Now $I = I_0 \exp\{-(\mu/\rho)x\}$, being μ/ρ the mass attenuation coefficient in cm^2/g.

If 2 pixels in the image have the same grey level, the same intensities have incised on the digitised X-ray plate. If one of them is beneath the bone we consider that it has received an intensity $I_h = I_0 \exp\{-(\mu/\rho)_h x_h\}$ and if the other is beneath the aluminium wedge then it has received $I_{Al} = I_0 \exp\{-(\mu/\rho)_{Al} x_{Al}\}$. Since $I_h = I_{Al}$, then it can be easily derived that

$$x_b(\mu/\rho)_b = x_{Al}(\mu/\rho)_{Al} \tag{9}$$

and from this expression the bone mass density (BMD) can be obtained since the parameters relative to the aluminium are known. $(\mu/\rho)_b$ and $(\mu/\rho)_{Al}$ are the mass attenuation coefficients in cm^2/g, and x_b and x_{Al} are the mass per area for bone and aluminium, in g/cm^2.

We use aluminium as reference material because the lineal attenuation coefficient mainly depends on the effective atomic number $Z_{eff}, Z_{Al} = 13$ for aluminium, and for the bone $Z_b = 12.5$. This means that both substances are characterised by similar attenuation spectra [22].

However, the X-ray beam is not monoenergetic and has a continuous spectrum that varies depending on the incising energy of the electrons emitted by the cathode. With the potential difference between the cathode–anticathode, we will control the penetration capability or beam hardness. For this, the Duane–Hunt law states the minimum wavelength (in angstroms) for the spectrum of this radiation as a function of the voltage in kilovolts applied to the tube, $\lambda_0 = 12.34/V$.

If a beam of 46 kV is provided, the threshold wavelength will be $\lambda_0 = 0.268$ Å. Having its intensity a maximum value of wavelength of $\lambda = 1.3\lambda_0$, most of the photons generated by the impact of the electrons against the anticathode nuclei will have an energy of $E = 3.55610^{-2}$ MeV. The mass attenuation coefficient of the photon mass for the aluminium will be $(\mu/\rho)_{Al} \cong 0.8$ cm^2/g at that energy.[2]

The aluminium wedge reference has known density and a calibrated shape (standard wedges are 4 cm length, 1 cm height, and angle of 22.5°). This way, we can compute the average grey level of the phalanx and compare it to the levels in the wedge image in order to establish how much thickness of aluminium corresponds to that level. Therefore, from the Eq. (10) we can establish a measurement in relation to the mass per area unit of the bone in adimensional arbitrary units (AU)

$$\mathrm{BMD}_{(AU)} = x_{Al}(\mu/\rho)_{Al} \tag{10}$$

4.1. Reliability of the measurements

To assess the reliability of the measurement obtained for comparing it to other standardised methods like DXA, it is necessary a repetitivity criterion. This means that the measurements performed have to be identical for different measures performed on the same object. This property is expressed through the variation coefficient, VC, and is defined as follows

$$\mathrm{VC} = \frac{\mathrm{Std\_dev}}{\mathrm{Mean}} \times 100 \tag{11}$$

This variation coefficient should be lower than 2% in order to have medical prognosis value. To observe this property, an exhaustive control on the different sources of error have to be evaluated when validating the method.

To assess the degree of variability of the measurements, three processes have to be clearly distinguished:

(1) The variability introduced by the algorithms in the border location. They affect the average grey level and, thus, the wedge width.
(2) The variability produced by the beam shot conditions, inherent to the radiographic plate and the operations involved for obtaining it. Here, also the variability introduced by the digitisation process is included.
(3) The comparison to other standardised methods looking for correlations in the BMD assessment.

The first aspect is analysed in Section 5, with a VC estimation on different convergences of the model on the data. For the second, we have tried to homogenise the shot conditions and will analyse, also in Section 5, the VC caused by all the variability sources involved. For the third, some bone density measurements obtained are compared below to those obtained through DXA using the *AccuDEXA* ® device.

5. Results

5.1. Shot condition and digitisation variability

We have homogenised the shot conditions because different beam hardness for the same hand generates a VC greater than 2%. A maximum radiologic contrast is desirable and, for this, voltage and amperage can be adjusted. These quantities are different for different parts of the body. After a number of tests in the ranges of 40–50 kV for voltage and

[2] The data of density and absorption coefficients for different substances (aluminium, bone, muscle, etc…) has been obtained from the NIST (National Institute of Standards and Technology, USA) http://physics.nist.gov/PhysRefData/XrayMassCoef/cover.html

1–3 mA for amperage, values of 46 kV and 2.5 mA have shown a good contrast for the hand images. Some spatial errors may appear due to the fact that the X-ray beam has a cone shape and, then, the air thickness traversed is different for different regions. To avoid this, the aluminium wedge is fixed to a solid template and a hand profile picture was drawn in order to make sure that the distance to the different hand phalanxes is constant for all the tests.

The radiographies were digitised using a high resolution scanner (*Duoscan Agfa T1200*) with a 180 ppi resolution and 8 bit grey level depth. The size of the images were 1256×1596 pixels. Higher resolutions were also tested but they do not improve the accuracy of the method significantly, while they multiply the amount of memory needed and the process time.

5.2. Phalanx and metacarpus segmentation

We have used the first 15 variation modes for the models to find a good fit to the contours (Fig. 4). Note that, in some cases, the model is attracted by edges belonging to different bones, especially in the metacarpal region. We have assumed this fact as an inaccuracy of the method and we will analyse how it conditions the precision and variability of the outcome.

Typically, a good convergence is achieved with less than 30 iterations. This implies a maximum of 1.5 s in a Pentium III at 500 MHz for the segmentation time, so the BMD can be assessed in real time.

The positioning of the initial shape is manually made clicking the mouse inside the bone image (black dots in

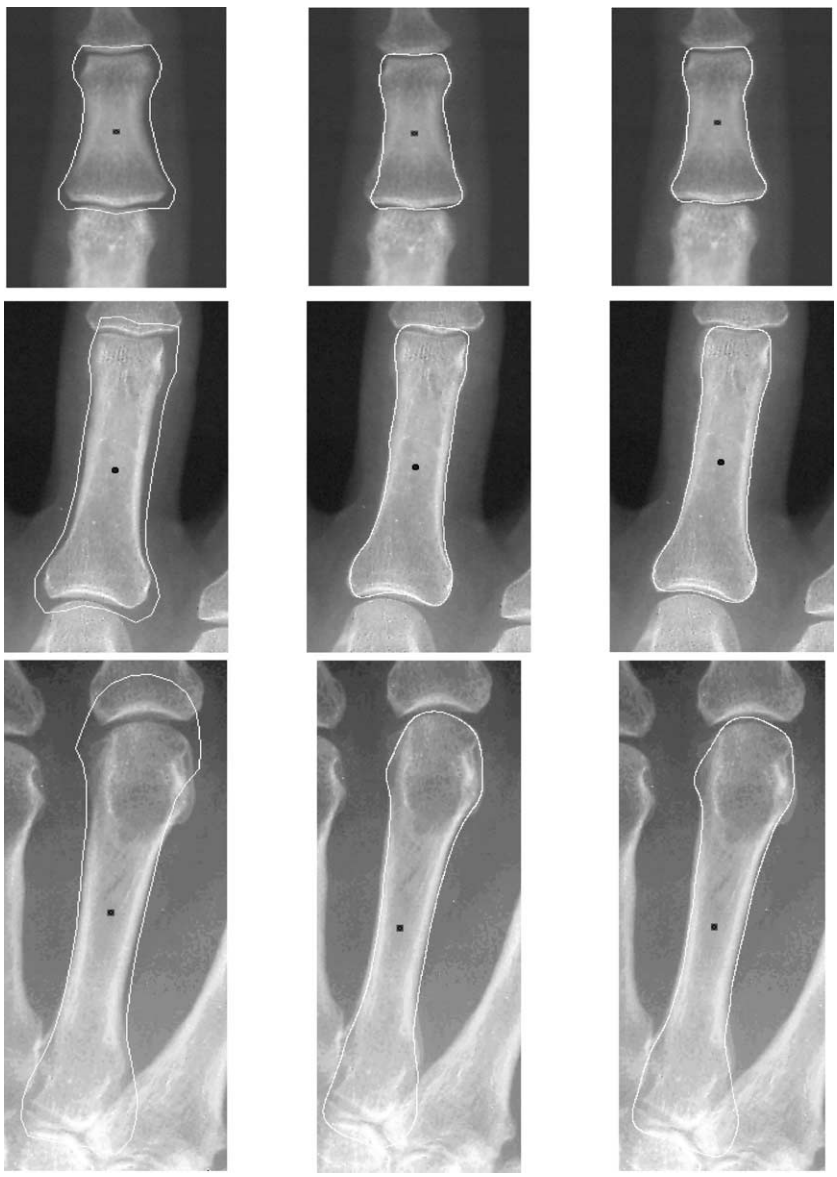

Fig. 4. Segmentation of the medial and proximal phalanxes, and metacarpus. (left) The active contours begin with the mean shape oriented with the same angle found for the finger. (center) Status of the model after five iterations, and (right) at the end of the process.

Table 2
Correlations of the BMD assessment among different bones and measurements using the proposed method

	Proximal phalanx	Medial phalanx	Metacarpus
Proximal phalanx	0.996		
Medial phalanx	0.917	0.986	
Metacarpus	0.908	0.816	0.986

Fig. 4). This generates a source of error that affects the model evolution, but it is needed as a guide to select the bone to be studied among all those present in the image. When the model does not find a better shape to approximate the candidate points we can say that the shape is well oriented respect its correct position. At that moment, the centre of mass is computed, the reference angle recalculated, and the initial errors are corrected (Fig. 4).

5.3. Repetitivity of the method

For assessing the reliability of the measurement obtained it is necessary a repetitivity criterion [6,23]. This means that the measurements performed should be identical in different measures performed on the same object. Two experiments have been designed to test this property of the method. Firstly, two different plates for 50 patients have been digitised and the BMD has been computed from them on different bones. The main difference between both tests was the initialisation of the ASM. The correlation coefficients were found to be very high as can be observed in Table 2.

The other experiment was the evaluation of the repetitivity of average grey level determination through the variation coefficient VC. Seventeen radiographs were scanned for five times in different days and the method was applied. A VC = 0.91% was found for medial phalanx, when the average grey level was determined from the whole surface of the segmented phalanx. For proximal phalanxes VC = 0.63%. For the third metacarpus VC = 1.19% using the average grey level determined in the central part of the phalanx in order to increase the accuracy. This higher variability for this bone is due to the problems in the convergence of the ASM described at the beginning of this section and observed in Fig. 4. Anyway, the VC still remains low in spite of the inaccuracy of the segmentation because the small error introduced is not critical.

5.4. Comparison to other standardised methods

To validate the data obtained through the new technique a comparative of different methods has been performed on 171 patients. The bone density measurements obtained for the proximal phalanx of one given finger for this set of patients was compared to those obtained through DXA phalanx measurement using the *AccuDEXA* ® device.

In Fig. 5 the results of the BMD measurement in those patients by our method and the *AccuDEXA* ® are displayed. After a linear regression, encouraging results were obtained, with a high linear correlation index of $r = 0.79$ that proves the reliability of the proposed method when compared with already accepted methodologies. Also this high correlation permits, from the linear regression analysis of the data, to establish a lineal relation between the measurements taken with *AccuDEXA* ® and with the proposed method, expressed as

$$\mathrm{DXA} = 0.586\,\mathrm{CXRA} - 0.171 \tag{12}$$

according to our data. This equation permits to estimate the value that would be achieved by *AccuDEXA* ® from the BMD assessed by our method.

The same experiment has been carried out also for other methods like the standard densitometry method (SDM)

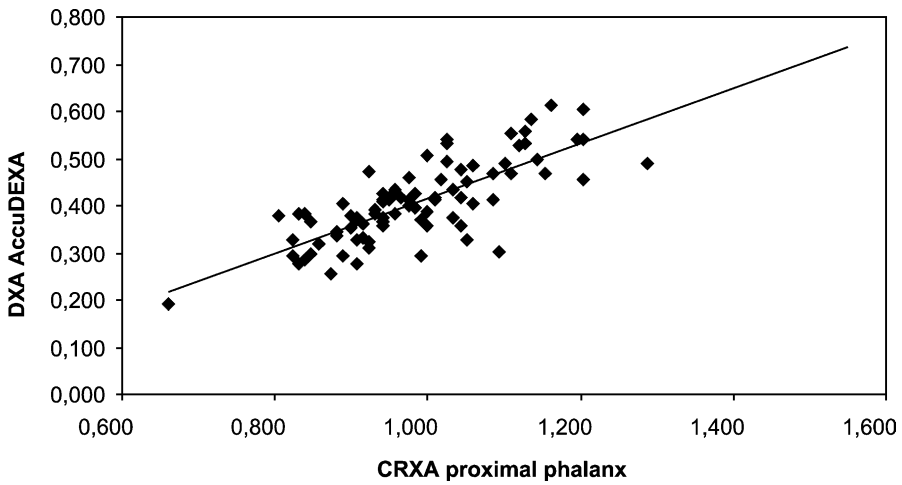

Fig. 5. Diagram of the linear correlation between the measurements obtained both with a commercial device in g/cm^2 and those obtained through our method (adim).

Table 3
Correlation indices for the different measurement devices. The proposed method for each bone considered appears like CXRA

	CXRA proxim.	CXRA medial	CXRA metac.	DXA	SDM lumbar	SDM hip
CXRA proxim.	1.0					
CXRA medial	0.89	1.0				
CXRA metac.	0.86	0.78	1.0			
DXA	0.79	0.73	0.72	1.0		
SDM lumbar	0.59	0.58	0.52	0.53	1.0	
SDM hip	0.65	0.57	0.58	0.64	0.73	1.0

applied to hip and lumbar spine with a *Lunar* ® device. The correlations obtained for the all the methods considered for all the patients are shown in Table 3. No repetitions with the same method have been carried out this time, so the diagonal shows $r = 1.0$ for all cases. Some of them show a not so high correlation, being the value of r reported above for *AccuDEXA* ® and CXRA proximal the best, apart from the correlations among the different bones using the proposed method.

The correlations between *AccuDEXA* ® and SDM are similar to those obtained when compared to our method, regardless of the bone considered. This high intra-method correlations and the low inter-method correlations point out that any method is valid for patient monitoring, but only if one uses always the same one.

6. Conclusions and future lines

An automatic hand bone segmentation method for radiographic images based on PDMs and deformable templates has been developed. The use of active curves and their variation modes for segmentation permits a precise location of the bone edges. This task is hard to solve with precision using traditional segmentation methods due both to the noise inherent to the medical images and the proximity of other bones. Once the contours of hand bones are located in hand radiographs, the average grey level in the region of interest is computed for assessing osteoporosis. The method fits the variability conditions (variability coefficient VC $< 2\%$) and correlation with well established methods like DXA ($r = 0.79$) as it is required to validate this new technique.

Our results indicate that this technique has an accuracy and repetitivity similar to DXA using *AccuDEXA* ®. The interest of our work is related to the possibility to determine the bone mineral density by means of conventional radiology techniques for a screening population system for osteoporosis assessment. In this way, a reliable and inexpensive test is obtained for selecting those patients that could be candidates for a standard DXA test.

One development line for the future could be to investigate if the results can be improved eliminating the hand muscle tissue attenuation in the segmented region, and study whether one or two shots are needed to do this. Also other studies can be directed to avoid the attraction of the models by edges belonging to different bones in order to make the segmentation more precise.

7. Summary

A system for osteoporosis screening has been developed. For applying such a system over a large population the system needs to avoid human measuring. The main problem for achieving a high standard of automation is the automatic segmentation of the bones of interest from digital radiographs. This problem has proved to be extremely challenging. The purposes of this work are: (1) to design a robust system to segment automatically hand bones in digitised radiographs of hands with a variability in the average grey level determination in the segmented area lower than 2%. For this, a PDM is generated from a set of training bone shapes. This technique permits to model the variation modes of a statistical model of the phalanx. These variation modes are also used to locate the boundaries of such bones, matching to the edges of each instance of the bones in the images with a high standard of precision; (2) to measure the bone density for the segmented hand bones, using their grey levels, calibrated with the absorption of the ray light intensity respect to a known substance, like aluminium, as a reference; (3) to design an accurate and reliable computerised radiographic X-ray absorptiometry system (CRXA) for automatic bone mass assessment that can be easily applied to the population; and (4) to validate the system and compare the results to other techniques and assess its diagnosis validity. The developed system has been tested and compared to other known methods with a high level of correlation.

Acknowledgements

This work has been funded by the Spanish ‘Ministerio de Sanidad y Consumo’ FISS grant 99/1147 and by the Spanish CICyT project TIC2000-1703-CO3-02.

References

[1] Proceedings of a symposium. Consensus Development Conference on Osteoporosis. October 19–20, 1990, Copenhagen, Denmark, Am J Med 1991;91(5B):1S–68S
[2] Hui SL, Slemenda CW, Johnston CC. Baseline measurement of bone mass predicts fracture in white women. Ann Intern Med 1989;III: 355–61.
[3] Barnett E, Nordin BEC. The radiological diagnosis of osteoporosis: a new approach. Clin Radiol 1960;11:166–74.
[4] Adami S, Zamberlan N, Gatti D, et al. Computed radiographic absorptiometry and morphometry in the assessment of postmenopausal bone loss. Osteoporos Int 1996;6(1):8–13.

[5] Seo GS, Shiraki M, Aoki C, et al. Assessment of bone density in the distal radius with computer assisted X-ray densitometry (CXD). Bone Miner 1994;27(3):173–82.
[6] Yang SO, Hagiwara S, Engelke K, et al. Radiographic absorptiometry for bone mineral measurement of the phalanxes: precision and accuracy study. Radiology 1994;192(3):857–9.
[7] Rico H, Revilla M, Villa LF, Martín-Santos JF, Cárdenas JL, Fraile E. Comparison between metacarpal bone measurements by computarized radiogrammetry and total body DEXA in normal and osteoporotic women. Clin Rheumatol 1994;13(4):593–7.
[8] Takada M, Engelke K, Hagiwara S, Grampp S, Jergas M, Gluer CC, Genant HK. Assessment of osteoporosis: comparison of radiographic absorptiometry of the phalanges and dual X-ray absorptiometry of the radius and lumbar spine. Radiology 1997;202(3):759–63.
[9] Swezey RL, Draper D, Swezey AM. Bone densitometry: comparison of dual energy X-ray absorptiometry to radiographic absorptiometry. J Rheumatol 1996;23(10):1734–8.
[10] Hayashi Y, Yamamoto K, Fukunaga M, Ishibashi T, Takahashi K, Nishii Y. Assessment of bone mass by image analysis of metacarpal bone roentgenograms: a quantitative digital image processing (DIP) method. Radiat Med 1990;8(5):173–8.
[11] Matsumoto C, Kushida K, Yamazaki K, Imose K, Inoue T. Metacarpal bone mass in normal and osteoporotic Japanese women using computed X-ray densitometry. Calcified Tissue Int 1994;55:324–9.
[12] Rucci M, Coppini G, Nicoletti I, Cheli D, Valli G. Automatic analysis of hand radiographs for the assessment of skeletal age: a subsymbolic approach. Comput Biomed Res 1995;28(3):239–56.
[13] Pietka E. Computer-assisted bone age assessment based on features automatically extracted from a hand radiograph. Comput Med Imag Graph 1995;19(3):251–9.
[14] Manos GK, Cairns AY, Rickets IW, Sinclair D. Segmenting radiographs of the hand and wrist. Comput Meth Prog Biomed 1994;43(3–4):227–37.
[15] Levitt TS, Hedgcock Jr. MW, Dye JW, Johnston SE, Shadle VM, Vosky D. Bayesian inference for model-based segmentation of computed radiographs of the hand. Artif Intell Med 1993;5(4):365–87.
[16] Fidouh F, Harba R, Jacquet G, Loussot T, Lespessailles E. Long-term reproducibility optimization of an X-ray process for bone architectural evaluation during osteoporosis. Phys Med Biol 1999;44(1):1–8.
[17] Cheng SN, Chan HP, Niklason LT, Adler RS. Automated segmentation of regions of interest on hand radiographs. Med Phys 1994;21(8): 1293–300.
[18] Seeger LL. Bone density determination. Spine 1997;22(24 Suppl.): 49S–57S.
[19] Cootes TF, Taylor CJ, Cooper DH, Graham J. Active shape models—their training and applications. Comp Vision Imag Understand 1995; 61(1):38–59.
[20] Efford ND. Knowledge-based segmentation and feature analysis of hand-wrist radiographs. Research Report 94.32. School of Comparative Studies, University of Leeds; 1994
[21] Kass M, Witkin A, Terzopoulos D. Snakes: active contour models. Proceedings of First International Conference on Computer Vision, IEEE Computer Society Press; 1987. p. 259–68.
[22] Kalebo P, Strid KG. Bone mass determination from microradiographs by computer-assisted videodensitometry. Acta Radiologica 1988;29: 611–7.
[23] Bouxsein ML, Michaeli DA, Plass DB, Schick DA, Melton ME. Precision and accuracy of computed digital absorptiometry for assessment of bone density of the hand. Osteoporos Int 1997;7(5): 444–9.

José Martínez Sotoca received a BSc degree in physics from the National University of 'Educación a Distancia' (UNED, Spain) in 1996 and the MSc degree in physics from the University of Valencia, Spain, in 1999. He received the PhD degree in physics also from the University of Valencia in 2001. Currently, he is Assistant Lecturer at the Department of Programming Languages and Computer Systems of the Jaume I University. His PhD work was on surface reconstructions with structured light. His main research interests lie in the area of pattern recognition and biomedical applications, including image pattern recognition, active contours, structured light, and feature extraction and selection.He has collaborated in different projects, most of them in medical applications of computer science, and has published around 20 scientific papers in national and international conferences, books and journals.

José Manuel Iñesta received a BSc degree in physics from the University of Valencia, Spain, in 1987 and a PhD also in physics from the same University. His PhD work was related to computer vision and measurement of medical structures. He was Assistant Lecturer in the Jaume I University of Castellón, Spain, and currently he is Professor of the Department of Programming Languages and Computer Systems of the University of Alicante, Spain, where he arrived in 1998. His main publications are seven books, 11 international journals, 14 book chapters, and more than 50 papers in international and national conferences. He has been involved in 19 research projects (national and international) covering medical applications of pattern recognition and artificial intelligence, robotics or digital libraries, among other lines of work. His main research interests range now from image analysis to pattern recognition algorithms with applications in medicine, robotics and computer music.

Miguel Ángel Belmonte graduated in medicine in 1980 at the Universitat Autonoma of Barcelona, Spain, and completed a doctorate in medicine in the same university in 1991, working on the developement and validation of a computer expert system to aid in arthropathies and collagen disease diagnosis. He trained in rheumatology at the Hospital de Bellvitge, in Barcelona, from 1982 to 1986. He is Consultant in rheumatology of the Hospital General de Castellón since 1987. He has been an Associate Professor in the Jaume I University, in Castellón, Spain, from 1994 to 1997. He is a member of the Spanish Society of rheumatology. He has published around 45 papers and his main research interests are outcomes in rheumatic diseases, cost-benefit analyses, databases, expert systems and fuzzy logic in medicine and web-based education applications.